Available online at www.sciencedirect.com
ScienceDirect
Journal of Power Sources 180 (2008) 561–567
JOURNAL OF POWER SOURCES
www.elsevier.com/locate/jpowsour

Diphenyloctyl phosphate and tris(2,2,2-trifluoroethyl) phosphite as flame-retardant additives for Li-ion cell electrolytes at elevated temperature

Tae-Heum Nam [a], Eun-Gi Shim [a], Jung-Gu Kim [a,*], Hyun-Soo Kim [b], Seong-In Moon [b]

[a] *Department of Advanced Materials Engineering, Sungkyunkwan University, Suwon 440-746, Republic of Korea*
[b] *Battery Research Group, Korea Electrotechnology Research Institute, Changwon 641-120, Republic of Korea*

Received 29 September 2007; received in revised form 12 November 2007; accepted 16 January 2008
Available online 7 February 2008

Abstract

The effect of diphenyloctyl phosphate (DPOF) and tris(2,2,2-trifluoroethyl) phosphite (TTFP) as flame-retardant (FR) additives in the liquid electrolyte of Li-ion cells is evaluated at both elevated temperature (40 °C) and room temperature (RT, 25 °C). The tested cells use mesocarbon microbeads (MCMB) and $LiCoO_2$ as the anode and cathode materials, respectively. Cell characteristics are investigated by means of electrochemical impedance spectroscopy (EIS) and scanning electron microscopy (SEM). The results of the cycle performance tests demonstrate the superior discharge capacity and capacity retention of the DPOF-containing cell compared will TTFP after cycling at both RT and 40 °C. Therefore, these results confirm the promising potential of DPOF as an FR additive for improving the electrochemical performance of Li-ion batteries.

Keywords: Li-ion battery; Electrolyte; Flame-retardant additives; Diphenyloctyl phosphate; Tris(2,2,2-trifluoroethyl) phosphite

1. Introduction

In comparison with other rechargeable batteries, the Li-ion battery is an attractive candidate as a power source for use in electric vehicles (EVs) and hybrid electric vehicles (HEVs) [1–4]. It does however, suffer some problems such as a safety hazard at elevated temperature, that must be overcome for the commercial application of high-power, Li-ion batteries in practical uses [4,5]. Safety hazards have been reported as being caused by chemical reactions between the electrode active materials and the electrolyte at elevated temperature [6–8]. To suppress the electrolytic flammability of Li-ion batteries, various flame-retardant (FR) additives have been investigated including tri(β-chloromethyl) phosphate (TCEP) [5], hexamethoxycyclotriphosphazene (HMPN) [9], 2,2-dimethoxy-propane (DMP) [10], hexamethylphosphoramide (HMPN) [11], ethylene ethyl phosphate (EEP) [12], and tris(2,2,2-trifluoroethyl) phosphite (TTFP) [13]. Zhang et al. [13] reported that TTFP is a promising FR additive due to its ability to reduce electrolyte flammability, and improve the cell performance [13].

In this study, the effect of diphenyloctyl phosphate (DPOF) and TTFP as flame-retardant additives on the cycle performance is evaluated at elevated temperature (40 °C) and room temperature (RT, 25 °C). Scanning electron microscopy (SEM) is used for morphological analyses of the electrodes after cycling tests, and electrochemical impedance spectroscopy (EIS) measurements for the change in internal impedance of the cells during the cycling testing.

2. Experimental

The cycling tests were performed using 2032 coin-type cells with an electrode diameter of 1.4 cm. In the Li-ion cell, mesocarbon microbeads (MCMB) and $LiCoO_2$ were used as the anode and cathode material, respectively. The electrolyte was 1.15 M $LiPF_6$ dissolved in a 3:7 mixture (by vol.%) of ethylene carbonate (EC) and ethylmethyl carbonate (EMC) as the blank electrolyte (E1). DPOF (E2) and TTFP (E3) were added at 5 wt.% to the blank electrolyte. The compositions of the three different electrolytes used are summarized in Table 1. A polypropylene, microporous membrane was used to separate the anode from the cathode. All cells were assembled in a dry room.

The cycling tests of the cells were performed at a charge–discharge rate of 1 C in the voltage range of 4.2–2.75 V for 30

* Corresponding author. Tel.: +82 31 2907360; fax: +82 31 2907371.
E-mail address: kimjg@skku.ac.kr (J.-G. Kim).

0378-7753/$ – see front matter © 2008 Elsevier B.V. All rights reserved.
doi:10.1016/j.jpowsour.2008.01.061

Table 1
Electrolyte compositions and cycle performance of three Li-ion cells after 30 cycles at RT and 40 °C

Temperature	Electrolyte no.	Compositions	Discharge capacity 1st cycle (mAh g^{-1})	Discharge capacity 30th cycle (mAh g^{-1})	Cycle performance (%)
RT	E1	1.15 M $LiPF_6$/EC:EMC (3:7, vol.%)	125.3	93.5	74.6
	E2	E1 + DPOF (5 wt.%)	121.6	94.1	77.4
	E3	E1 + TTFP (5 wt.%)	116.8	73.5	62.9
40 °C	E1	1.15 M $LiPF_6$/EC:EMC (3:7, vol.%)	125.6	95.0	75.6
	E2	E1 + DPOF (5 wt.%)	122.7	102.5	83.5
	E3	E1 + TTFP (5 wt.%)	120.1	79.8	66.4

cycles at 40 °C and RT. The tests were carried out with a VMP2 system. The impedance of the cells after charging (4.2 V) at the 1st, 10th, 20th and 30th cycles was determined with the VMP2 system. The frequency was varied from 100 kHz to 10 mHz and the amplitude was set at 10 mV. The impedance data were analyzed using ZSimpWin Version 3.00 software. To investigate the morphology of the electrode surface, the samples were subjected to scanning electron microscopic (SEM) observation after 30 cycles.

3. Results and discussion

The cycling results of the cells with the three different electrolytes at RT and 40 °C are shown in Figs. 1 and 2, and Table 1. As shown in Fig. 1, the discharge capacities of the three cells decrease with increasing cycle number. In particular, the TTFP-containing cell gives an inferior discharge capacity after 30 cycles. The cell with DPOF (94.1 mAh g^{-1}) shows a slightly higher discharge capacity than either the blank electrolyte cell (93.5 mAh g^{-1}) or the TTFP-containing cell (73.5 mAh g^{-1}) after 30 cycles. In cycle performance, the cells with blank electrolyte, DPOF and TTFP exhibited a capacity retention of about 75, 77, and 63% of the initial capacity after 30 cycles, respectively. This confirms the superior cycle performance at RT of the DPOF-containing cell among the three electrolytes at RT.

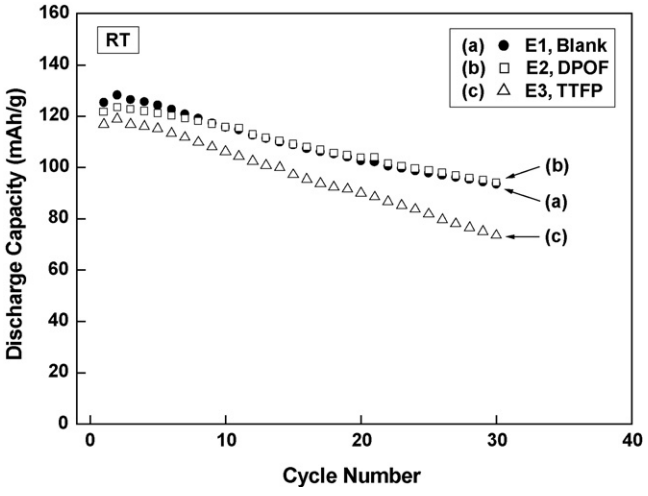

Fig. 1. Cycle performance of Li-ion cells with different electrolytes at RT: (a) blank electrolyte; (b) blank electrolyte + DPOF; (c) blank electrolyte + TTFP.

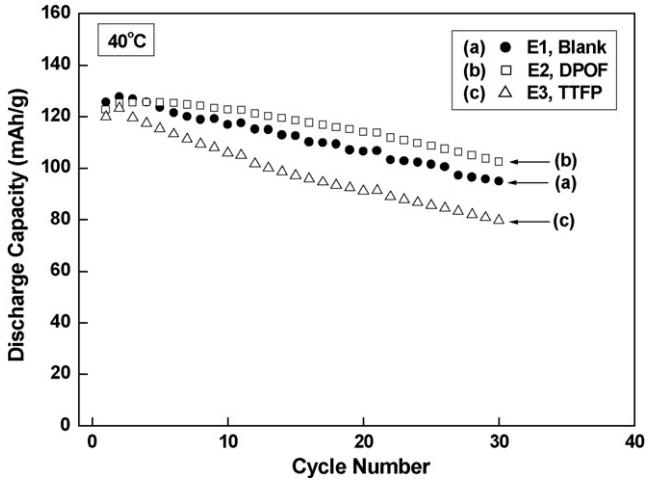

Fig. 2. Cycle performance of Li-ion cells with different electrolytes at 40 °C: (a) blank electrolyte; (b) blank electrolyte + DPOF; (c) blank electrolyte + TTFP.

Fig. 2 shows the cycling behaviour of the cells at 40 °C. The DPOF-containing cell (102.5 mAh g^{-1}) has a higher discharge capacity than the blank electrolyte cell (95.0 mAh g^{-1}) and the TTFP-containing cell (79.8 mAh g^{-1}) after 30 cycles. The cells

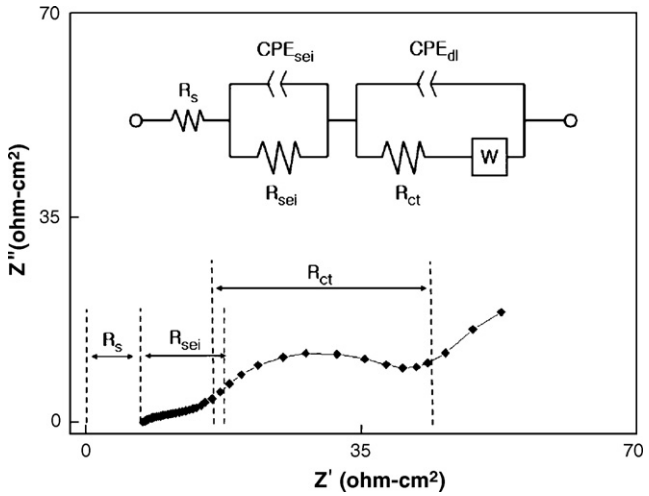

Fig. 3. Equivalent circuit used for EIS analyses and typical EIS results for the Li-ion cell.

with blank electrolyte, DPOF and TTFP exhibited a capacity retention of about 76, 84, and 66% of the initial capacity after 30 cycles, respectively, and this further confirms the superior cycle performance of the cell with DPOF-containing electrolyte at 40 °C. A comparison of Figs. 1 and 2 demonstrates the improved cycle performance of the cells at 40 °C compared with that at RT, and the superior cycle performance of the DPOF-containing cell at both RT and 40 °C. The improved cycleability has been attributed to a decrease in the internal impedance of the cells during cycling [2–4,14].

The change in the electrochemical impedance of each cell was measured during 30 cycles. A typical EIS result for the Li-ion cell and the equivalent circuit used for EIS analysis are given in Fig. 3, in which R_s is the cell electrolyte resistance at high fre-

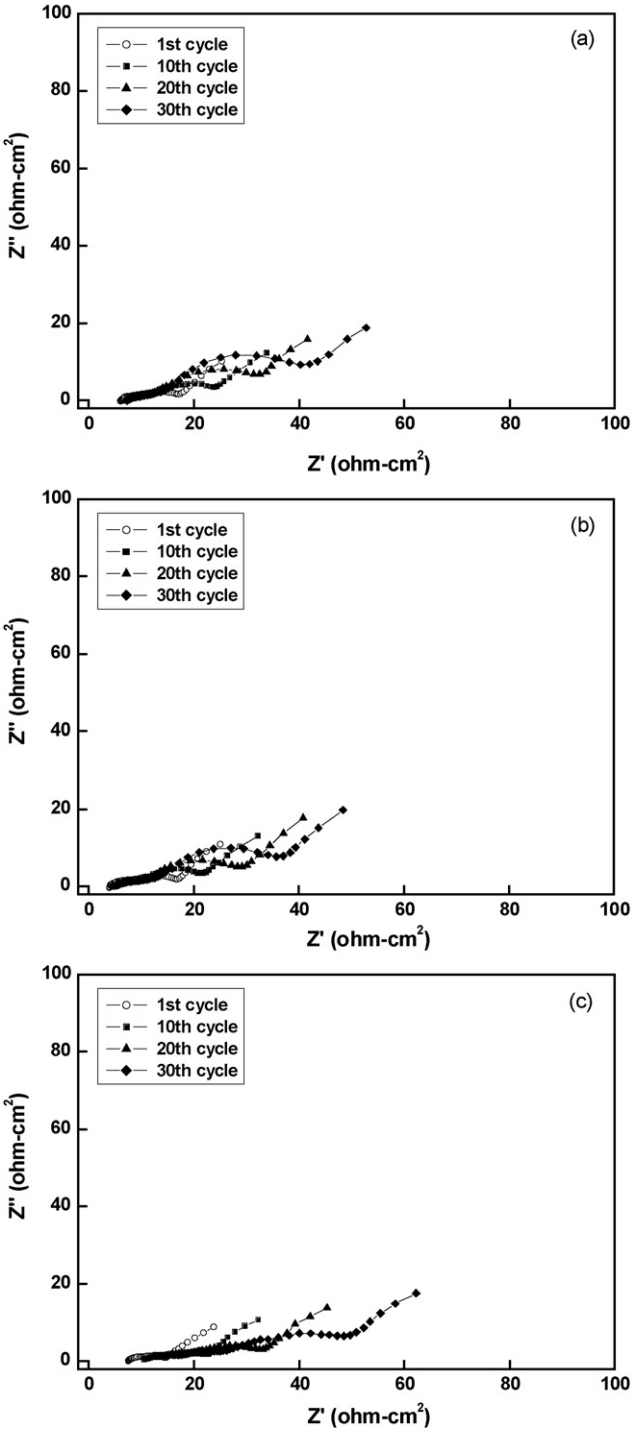

Fig. 4. Nyquist plots of Li-ion cells with different electrolytes at 1st, 10th, 20th, and 30th cycle at RT: (a) blank electrolyte; (b) blank electrolyte + DPOF; (c) blank electrolyte + TTFP.

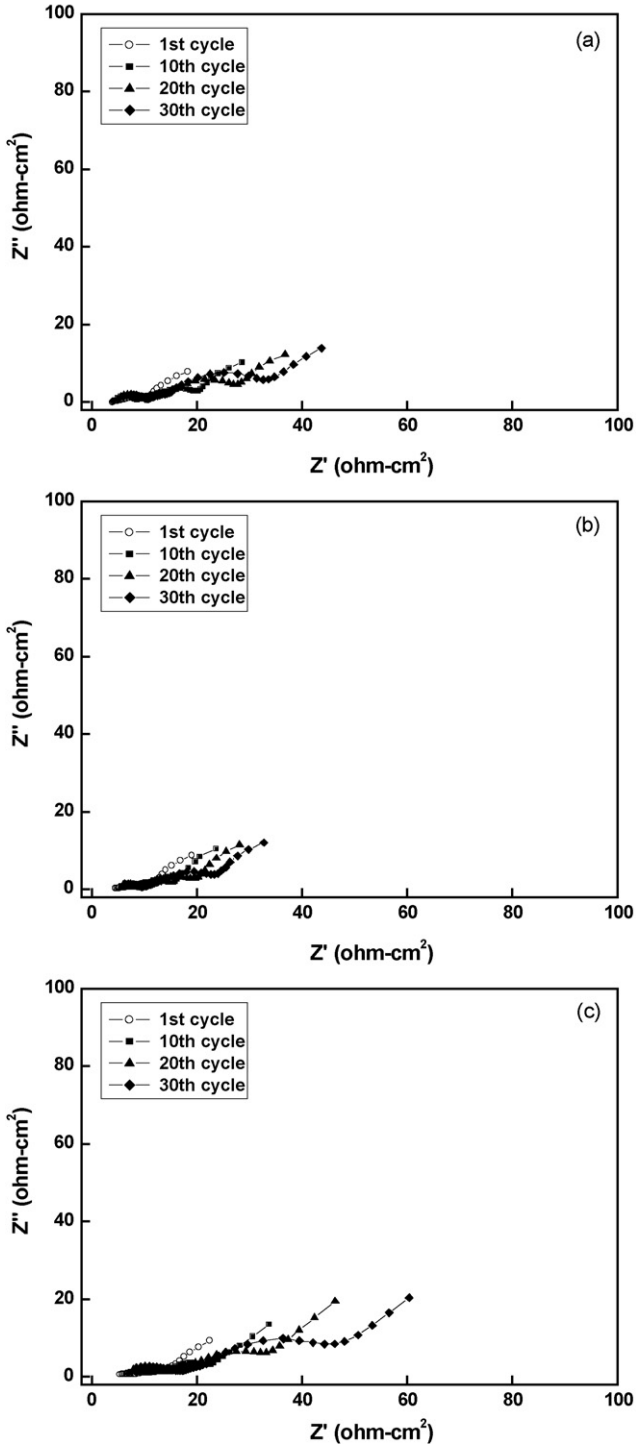

Fig. 5. Nyquist plots of Li-ion cells with different electrolytes at 1st, 10th, 20th, and 30th cycle at 40 °C: (a) blank electrolyte; (b) blank electrolyte + DPOF; (c) blank electrolyte + TTFP.

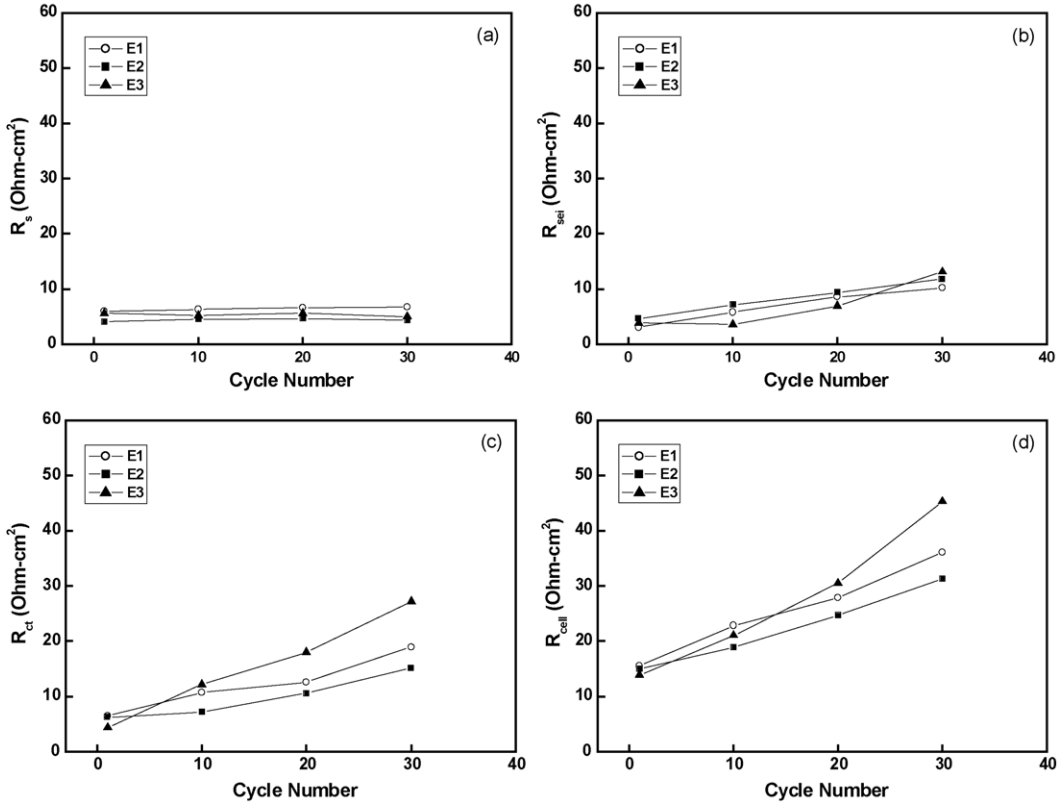

Fig. 6. EIS fitting parameters of Li-ion cells with different electrolytes at the 1st, 10th, 20th, and 30th cycle at RT: (a) R_s; (b) R_{sei}; (c) R_{ct}; (d) R_{cell}.

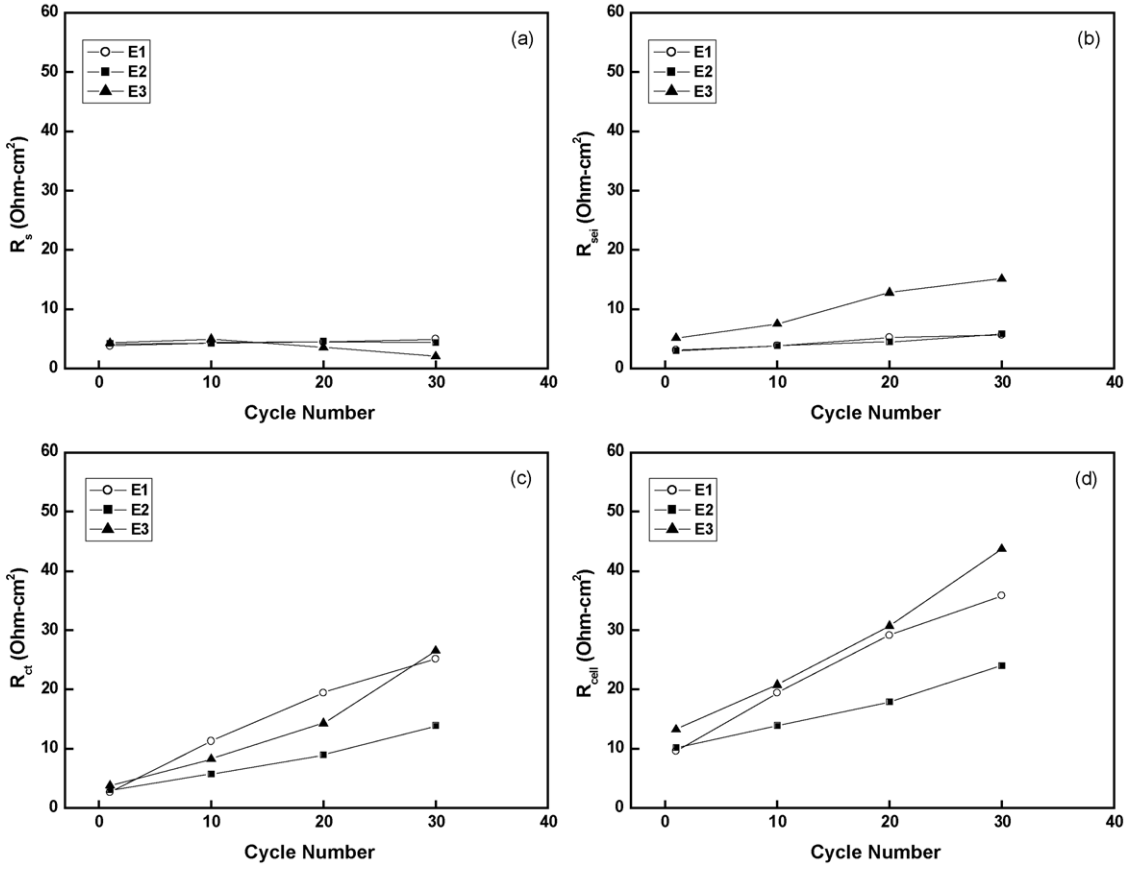

Fig. 7. EIS fitting parameters of Li-ion cells with different electrolytes at the 1st, 10th, 20th, and 30th cycle at 40 °C: (a) R_s; (b) R_{sei}; (c) R_{ct}; (d) R_{cell}.

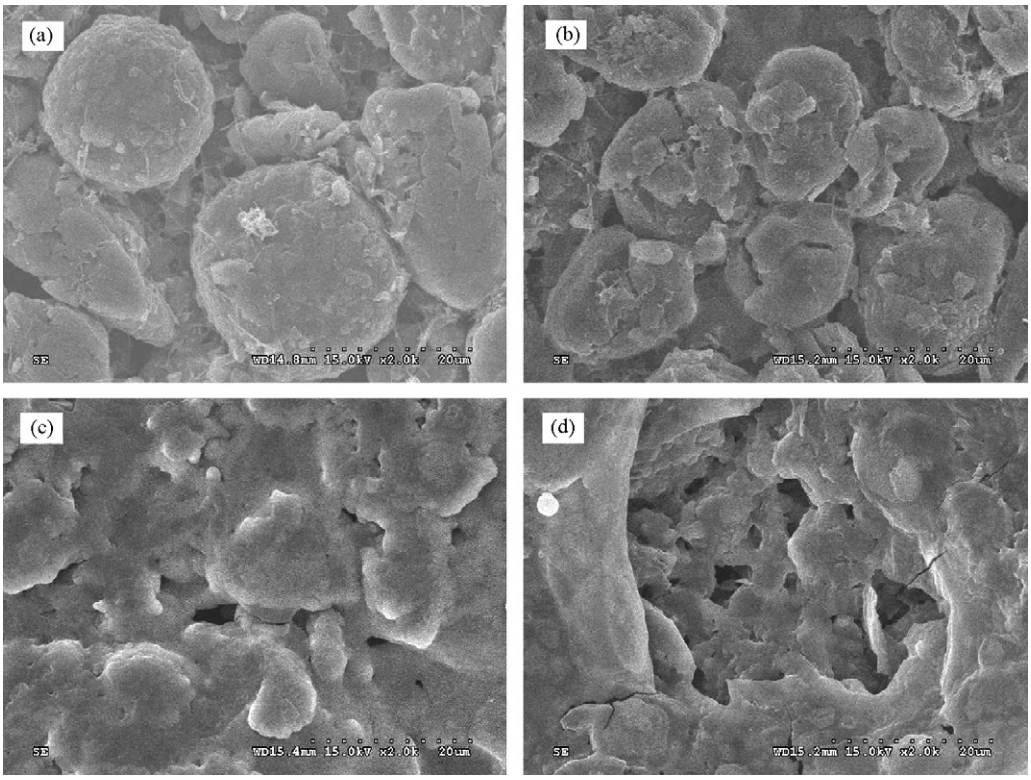

Fig. 8. Scanning electron micrographs of MCMB electrodes with different electrolytes after 30 cycles at RT: (a) pristine electrode; (b) blank electrolyte; (c) blank electrolyte + DPOF; (d) blank electrolyte + TTFP.

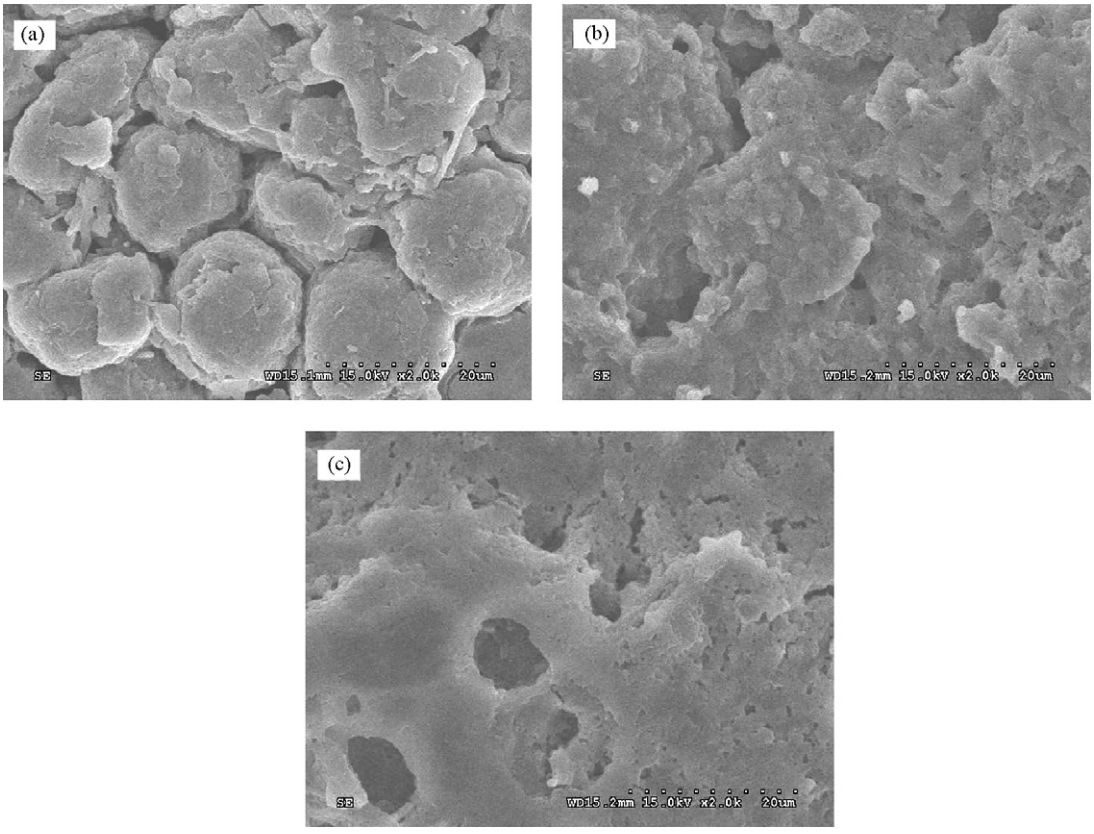

Fig. 9. Scanning electron micrographs of MCMB electrodes with different electrolytes after 30 cycles at 40 °C: (a) blank electrolyte; (b) blank electrolyte + DPOF; (c) blank electrolyte + TTFP.

quency, while R_{sei} at middle frequency and R_{ct} at low frequency are the resistances of the solid electrolyte interface (SEI) film and the charge-transfer resistance, respectively. CPE_{sei} and CPE_{dl} are the constant-phase elements (CPEs) corresponding to the SEI capacitance and electric double-layer capacitance, respectively. CPEs are electric elements which indicate the shape of the depressed capacitive loop, and it has been suggested that the capacitance dispersion is caused by the electrode roughness and the porous structure. W is the Warburg impedance related to the diffusion of lithium ions at the interface between the active material particles and the electrolyte, and corresponds to the straight sloping line at the low frequency end [14–17]. Figs. 4 and 5 show the impedance curves measured after charging (4.2 V) during cycling at RT and 40 °C, respectively. The cell impedance increases with cycle number.

Usually, an increase in cell impedance with cycling is due to non-uniformity of the SEI film, electrolyte decomposition, current-collector corrosion, and/or phase segregation in the cathode [2]. Zhang et al. [18] reported that the total resistance ($R_{cell} = R_s + R_{sei} + R_{ct}$) of a Li-ion cell is mainly composed of the bulk (R_b), solid-state interface (R_{sei}), and charge-transfer (R_{ct}) resistances. The R_{cell} value of the Li-ion cell is predominately determined by the R_{ct} value, which reflects the kinetics of the cell reactions. Figs. 6 and 7 present the fitted values of R_s, R_{sei}, R_{ct}, and R_{cell} per cycle as a function of cycle number at RT and 40 °C, respectively. The total resistance (R_{cell}), and especially R_{ct}, of the cells show a larger increase than of R_s and R_{sei} after 30 cycles. The R_{cell} of the cell with DPOF (31.3 Ω cm^2) was smaller than that with TTFP (45.3 Ω cm^2) after 30 cycles at RT (Fig. 6), due to the decrease of R_s, R_{sei} and, especially, R_{ct}. The R_{cell} value of the cell with TTFP (43.7 Ω cm^2) was larger than that with DPOF (24.0 Ω cm^2) after 30 cycles at 40 °C (Fig. 7), due to the increase of R_{sei} and especially R_{ct}. These results seem to indicate that the capacity fading of the cell with TFPP was caused by the increase in R_{cell}, especially R_{ct}, in the cell impedance during cycling at both RT and 40 °C.

The formation of a low-impedance SEI film is not only important for enhancing the cell performance but also for reducing electrolyte decomposition [19]. Comparing Figs. 6(b) and 7(b), the R_{sei} values of the cell with DPOF (11.8 and 5.8 Ω cm^2) were smaller than those with TTFP (13.1 and 15.1 Ω cm^2) after 30 cycles at RT and 40 °C, respectively. These results show that R_{sei} of the cell with DPOF at 40 °C (5.8 Ω cm^2) is smaller than that at RT (11.8 Ω cm^2). Comparing Figs. 6 and 7, R_{cell} at RT is higher than R_{cell} at 40 °C, because the impedance of the Li-ion cells is reduced with increasing test temperature [16]. The DPOF-containing cell exhibited the lowest impedance of R_{cell} at both RT and 40 °C. The comparison of the above cycling and EIS test results (Figs. 6–7) indicate that the DPOF-containing cell exhibits a higher discharge capacity and lower impedance than that of TTFP-containing cell after 30 cycles at both RT and 40 °C. In this regard, the EIS and cycling test results are complementary.

In order to investigate the effect of the additive on electrode morphology after 30 cycles at RT and 40 °C, SEM micrographs of the MCMB electrodes are shown in Figs. 8 and 9, respectively. The micrographs of the electrodes cycled and DPOF and TTFP reveal a very different topography than the cycled with a

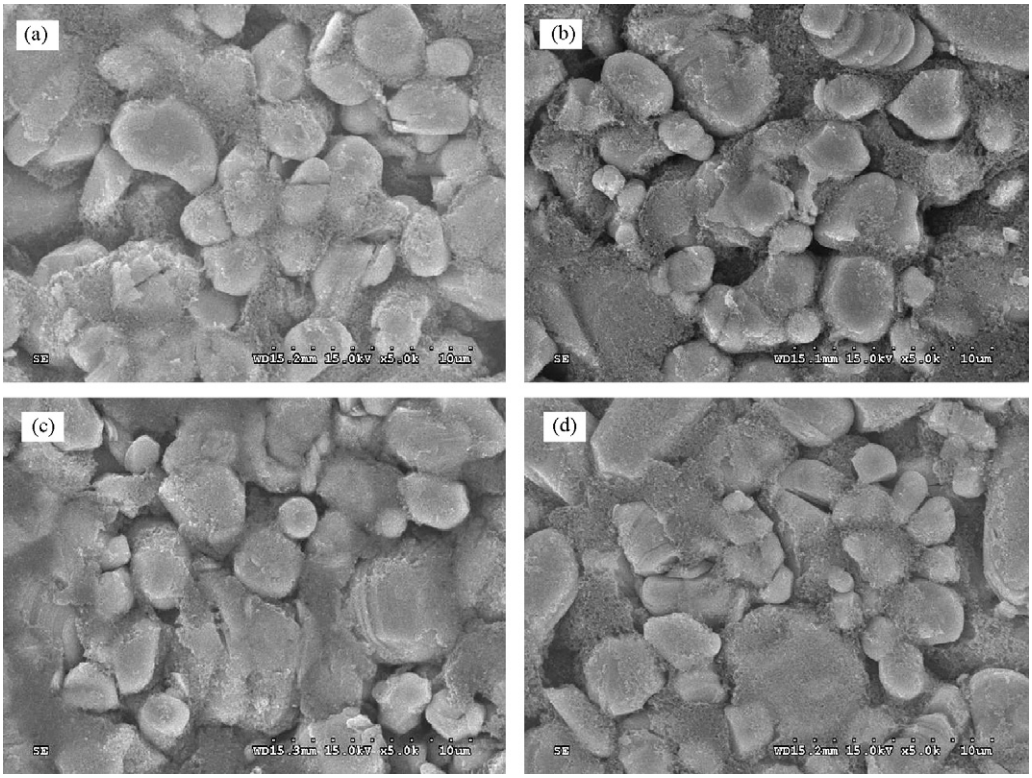

Fig. 10. Scanning electron micrographs of $LiCoO_2$ electrodes with different electrolytes after 30 cycles at RT: (a) pristine electrode; (b) blank electrolyte; (c) blank electrolyte + DPOF; (d) blank electrolyte + TTFP.

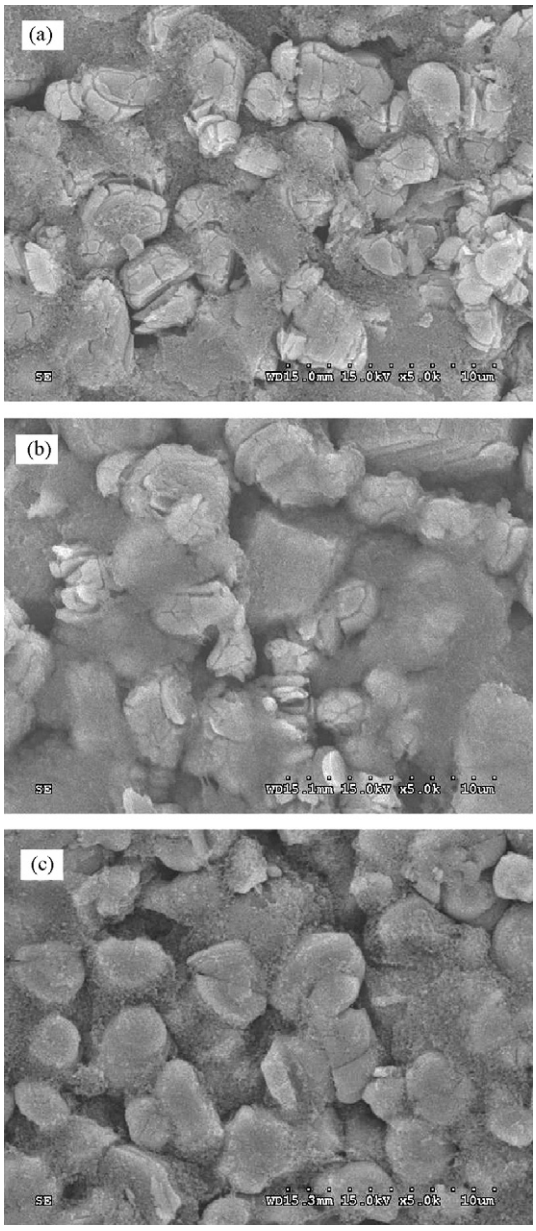

Fig. 11. Scanning electron micrographs of $LiCoO_2$ electrodes with different electrolytes after 30 cycles at 40 °C: (a) blank electrolyte; (b) blank electrolyte + DPOF; (c) blank electrolyte + TTFP.

blank electrolyte. The DPOF- and TTFP-containing electrodes are completely covered with a thick SEI film at both RT and 40 °C. The aforementioned EIS test results (Figs. 6(b) and 7(b)) indicate that the R_{sei} value of the cell with DPOF at 40 °C represents a lower impedance SEI film than that at RT from these results, the SEI film on the DPOF-containing electrode at 40 °C is more stable than that at RT, as shown in Figs. 8(c) and 9(b). It is assumed that the thick film of the DPOF-containing electrode is derived from the diphenyl [20,21] of the DPOF additive used in this study.

Figs. 10 and 11 show SEM micrographs of the $LiCoO_2$ electrode obtained from the cell after 30 cycles at RT and 40 °C, respectively. The electrodes cycled with DPOF and TTFP are covered with a thin film, which is significantly different from the thick surface film on the MCMB anode of Figs. 8 and 9. In addition, the SEM micrographs of the electrodes cycled at 40 °C present very different shape than that at RT, as demonstrated in Figs. 10 and 11. This indicates that the particles on the $LiCoO_2$ electrode at 40 °C are more crushed than those at RT, and is attributed to the increased in cell temperature.

4. Conclusions

This study examines the cell performance of two FR additives, DPOF and TTFP, in a liquid electrolyte of Li-ion cells. In cycling performance tests, the cell with the DPOF additive yields better capacity retention and discharge capacity than those with TTFP and the blank electrolyte after cycling at both RT and 40 °C. Also, the performance and discharge capacity of all three cells are better at 40 °C than at RT. These results confirm the improved cycleability of the DPOF-containing cell, because the internal impedance of the cell is decrease after cycling, and the superiority of DPOF over TTFP as an FR electrolyte additive for Li-ion batteries.

Acknowledgement

The supply of electrolytes by TECHNO SEMICHEM Co. Ltd. is gratefully acknowledged.

References

[1] Y.E. Hyung, S.I. Moon, D.H. Yum, S.K. Yun, J. Power Sources 81 (1999) 842.
[2] J. Shim, R. Kostecki, T. Richardson, X. Song, K.A. Striebel, J. Power Sources 112 (2002) 222.
[3] J.R. Belt, C.D. Ho, T.J. Miller, M.A. Habib, T.Q. Duong, J. Power Sources 142 (2005) 354.
[4] B. Kennedy, D. Patterson, S. Camilleri, J. Power Sources 90 (2000) 156.
[5] Y.B. He, Q. Liu, Z.Y. Tang, Y.H. Chen, Q.S. Song, Electrochim. Acta 52 (2007) 3534.
[6] M.N. Richard, J.R. Dahn, J. Electrochem. Soc. 146 (1999) 2078.
[7] H. Maleki, G. Deng, A. Anani, J. Howard, J. Electrochem. Soc. 146 (1999) 3224.
[8] M.N. Richard, J.R. Dahn, J. Electrochem. Soc. 146 (1999) 2068.
[9] C.W. Lee, R. Venkatachalapathy, J. Prakash, Electrochem. Solid-State Lett. 3 (2000) 63.
[10] C.C. Chang, L.J. Her, L.C. Chen, Y.Y. Lee, S.J. Liu, H.J. Tien, J. Power Sources 163 (2007) 1059.
[11] S.I. Gonzales, W. Li, B.L. Lucht, J. Power Sources 135 (2004) 291.
[12] H. Ota, A. Kominato, W.J. Chun, E. Yasukawa, S. Kasuya, J. Power Sources 119-121 (2003) 393.
[13] S.S. Zhang, K. Xu, T.R. Jow, J. Power Sources 113 (2003) 166.
[14] D.P. Abraham, E.M. Reynolds, P.L. Schultz, A.N. Jansen, D.W. Dees, J. Electrochem. Soc. 158 (2006) A1610.
[15] S. Yang, H. Song, X. Chen, Electrochem. Commun. 8 (2006) 137.
[16] S. Zhang, M.S. Ding, K. Xu, J. Allen, T.R. Jow, Electrochem. Solid-State Lett. 4 (2001) A206.
[17] M. Itagaki, N. Kobari, S. Yotsuda, K. Watanabe, S. Kinoshita, M. Ue, J. Power Sources 148 (2005) 78.
[18] S.S. Zhang, K. Xu, T.R. Jow, Electrochim. Acta 49 (2004) 1057.
[19] K. Abe, H. Yoshitake, T. Kitakura, T. Hattori, H. Wang, M. Yoshio, Electrochim. Acta 49 (2004) 4613.
[20] K. Abe, Y. Ushigoe, H. Yoshitake, M. Yoshio, J. Power Sources 153 (2006) 328.
[21] K. Shima, K. Shizuka, M. Ue, H. Ota, T. Hatozaki, J.I. Yamaki, J. Power Sources 161 (2006) 1264.